

The signature of dissipation in the mass-size relation: are bulges simply spheroids wrapped in a disc?

Trystyn A. M. Berg¹, Luc Simard², J. Trevor Mendel³, Sara L. Ellison¹

¹*Department of Physics and Astronomy, University of Victoria, Victoria, BC, V8W 2Y2, Canada*

²*National Research Council of Canada, 5071 West Saanich Road, Victoria, BC, V9E 2E7, Canada*

³*Max Planck Institut für Extraterrestrische Physik, Giessenbachstraße, D-85748 Garching, Germany*

2 April 2022

ABSTRACT

The relation between the stellar mass and size of a galaxy’s structural subcomponents, such as discs and spheroids, is a powerful way to understand the processes involved in their formation. Using very large catalogues of photometric bulge+disc structural decompositions and stellar masses from the Sloan Digital Sky Survey Data Release Seven, we carefully define two large subsamples of spheroids in a quantitative manner such that both samples share similar characteristics with one important exception: the ‘bulges’ are embedded in a disc and the ‘pure spheroids’ are galaxies with a single structural component. Our bulge and pure spheroid subsample sizes are 76,012 and 171,243 respectively. Above a stellar mass of $\sim 10^{10} M_{\odot}$, the mass-size relations of both subsamples are parallel to one another and are close to lines of constant surface mass density. However, the relations are offset by a factor of 1.4, which may be explained by the dominance of dissipation in their formation processes. Whereas the size-mass relation of bulges in discs is consistent with gas-rich mergers, pure spheroids appear to have been formed via a combination of ‘dry’ and ‘wet’ mergers.

Key words: galaxies: bulges – galaxies: evolution – galaxies: elliptical and lenticular, cD

1 INTRODUCTION

The structure of galaxies emerges from a complex process of hierarchical mass assembly in which mergers and other processes such as dissipation play key roles. Discs and spheroids contain the bulk of the light (and thus stellar mass) of galaxies, and their scaling relations encode valuable information about their formation and evolution (e.g. Fall & Efstathiou 1980; Djorgovski & Davis 1987; Burstein, Bender, & Faber 1997; Mo, Mao, & White 1998). Discs and spheroids have been most often distinguished on the basis of photometric data from which light profiles are measured and morphological decompositions are performed (e.g. Freeman 1970; Borson 1981; Kent 1985; de Jong 1996; Peng et al. 2002; Simard et al. 2002, 2011; Lackner & Gunn 2012; Meert et al. 2013). Under this observational classification paradigm, spheroids are parametrically described by Sérsic/de Vaucouleurs light profiles, whereas discs’ profiles follow an exponential decline. However, this relatively simple picture is changing with the greater availability of detailed internal kinematics data, e.g., ATLAS^{3D} (Krajnović et al. 2012). Through comparisons between photometric and kinematical data, fast rotators have been associated with disc galaxies and slow rotators with dispersion-supported spheroids. The fast/slow rotator classification is also closer to the definition of structure in nu-

merical simulations (e.g. Abadi et al. 2003; Governato et al. 2007; Hopkins et al. 2009a; Agertz et al. 2011; Brooks et al. 2011; Scannapieco et al. 2011). High angular momentum particles in these simulations are associated with a disc, and spheroids comprise the low angular momentum particles.

An extensive body of theoretical and observational studies (e.g., Bender, Burstein, & Faber 1992; Ciotti & van Albada 2001; Shen et al. 2003; Robertson et al. 2006; Ciotti et al. 2007; Scarlata et al. 2007; Hopkins et al. 2009a; Nipoti, Treu, & Bolton 2009; Auger et al. 2010; Nipoti et al. 2012; Shankar et al. 2013; Taranu et al. 2013) has shown that merger histories and hydrodynamical processes such as dissipation shape the properties of spheroids. Much of this work has focused on reproducing the mass-size relation. This fundamental relation describes how the sizes of galaxies scale with their stellar mass. The relation is a projection of the Fundamental Plane (Djorgovski & Davis 1987), an inherent relation for all dispersion supported galaxies and is typically very tight (e.g. Lauer et al. 2007; Kormendy et al. 2009). However, there are interesting trends that remain to be studied in greater detail. For example, Shen et al. (2003) found that the merger of two similar late-type galaxies produced an apparent flattening of the mass-size relation of the remnant spheroid and that disc instabilities were responsible

for growing the bulge. Shankar et al. (2013) found a similar flattening, but they attributed it to the lack of gas in the merging galaxies. There is also evidence that bulges are not present-day elliptical galaxies embedded in discs (Graham & Worley 2008; Gadotti 2009; Gadotti & Kauffmann 2009; Laurikainen et al. 2010) as they exhibit different mass-size relations.

The gas content of a merger progenitor can determine the size of the virialized remnant as it controls the amount of energy that can be lost as a result of dissipation. Gas-rich (‘wet’) mergers tend to dissipate orbital energy, which shrinks the effective size of the system as the gas cools. The light profile of such a galaxy will have a higher stellar surface density due to the increasing central concentration of stars (Hopkins et al. 2009b, and references therein). However gas-poor (‘dry’) mergers maintain this energy in stellar orbits, keeping the galaxy puffed up. Violent relaxation can mimic dry mergers by ejecting stars into the outer regions of galaxies, making the light profile extend to larger radii. Discs can regrow and be replenished around these merger remnants both by diffuse infall from the surroundings and by gas accreted from satellite galaxies (e.g. Guo et al. 2011). Although one might expect discs to be destroyed in the merging process itself, both Robertson et al. (2006) and Hopkins et al. (2009b) (amongst others) demonstrated that discs can quickly reform during the merger with sufficiently gas-rich progenitor galaxies. The bulge is then built very slowly with little angular momentum, keeping it small. Finally, the bulge component of disc galaxies can also form via secular instabilities in the disc, transferring some disc material into the bulge component (Courteau et al. 1996; Shen et al. 2003, and references therein).

Shankar et al. (2013) have recently demonstrated with semi-analytic models of galaxy evolution (Guo et al. 2011) that the mass-size relation flattens for spheroidal galaxies formed by *dissipationless* processes below a critical mass of $\sim 10^{11} M_{\odot}$. This result differs from their sample of observations of early-type galaxies from the Sloan Digital Sky Survey (SDSS). The pure power law description of their data was suggested to be the result of *dissipation* of energy due to wet mergers. The flattening effect seen below a critical mass is believed to be an event of dry mergers as the excess energy puffs up the spheroidal component of the galaxy. Hopkins et al. (2009b) also simulated several mergers of different masses and different gas contents. They found that when dry mergers are turned off (i.e. only wet mergers); the sizes are much smaller than expected, although the mass-size relation still remains more or less a power law. When gas was treated like stars (i.e. no dissipation), a power law similar to the ‘no dry merger’ case resulted; however, these sizes are larger than those from wet mergers. These two studies show that the size of the bulges in gas-rich galaxies seems to be smaller than their dry-merging counterparts. However, both pieces of work disagree on how strong the effects of dissipation are as their mass-size relations are inconsistent with each other, especially with the flattening seen by Shankar et al. (2013) at low masses.

In order to better understand the effects of dissipation on the formation of the spheroidal components of galaxies, we study the mass-size relations of two very large spheroidal subsamples, namely bulges and pure spheroids, and compare them with expectations from theoretical models. The care-

ful, quantitative selection of our subsamples, derivation of spheroid masses and the characterization of the mass-size relation are described in Section 2. Our results are discussed in Section 3. The cosmology adopted throughout this paper is $(H_0, \Omega_m, \Omega_{\Lambda}) = (70 \text{ km s}^{-1} \text{ Mpc}^{-1}, 0.3, 0.7)$.

2 DATA

2.1 Sample Selection

The taxonomy of describing galaxy subcomponents in the literature is quite diverse. In addition to galaxy discs, the literature is filled with pseudo-bulges, classical bulges, lenticulars, and spheroidals just to name a few (Kormendy & Bender 2012). We adopt ‘spheroid’ here to describe the structural component of a galaxy that is not a disc (and not a bar). Spheroids can then be divided into two categories: bulges which are spheroids embedded in discs and pure spheroids which correspond to single component galaxies. We seek to quantitatively define bulge and pure spheroid subsamples by applying a set of selection criteria to the large catalogues of $n = 4$ bulge+disc decompositions and stellar masses presented by Simard et al. (2011) (S11 hereafter) and Mendel et al. (2014) (M14 hereafter) for spectroscopically-observed galaxies in the Legacy area of the SDSS Data Release Seven (Abazajian et al. 2009). Even though the parameters of the S11 decompositions do match those measured from deeper, higher resolution observations (e.g. Kanwar et al. 2008); the spatial resolution of SDSS images is unfortunately insufficient over the magnitude range of our sample to accurately measure the Sérsic index of the bulge itself. We therefore cannot differentiate between different kinds of bulge profiles. Furthermore, our photometric decompositions cannot differentiate between virially-supported or disc-like (e.g. Cappellari et al. 2011) structures without any kinematic data.

We start by selecting galaxies with effective r -band surface brightness $\mu_{50,r} \leq 23.0 \text{ mag arcsec}^{-2}$, SDSS data base flag `Specclass` = 2 and spectroscopic redshifts in the range $0.005 \leq z \leq 0.2$. The cut on surface brightness was necessary as fainter galaxies up to $24 \text{ mag arcsec}^{-2}$ were only targeted when the global and local sky values were within 0.5 mag of each other. The `Specclass` flag selects objects that have been identified as galaxies on the basis of their spectral energy distribution. The redshift selection ensures that peculiar velocities do not dominate the distance determination of galaxies in our sample. We applied a quality control criterion to our SDSS catalogues. We used Δ_{B+D} to keep only galaxies for which the sum of their individual bulge and disc masses is within 3σ of their total stellar mass as a consistency check (as discussed in M14).

M14 discuss the classification of galaxies based on their 1D profiles into one of four types: (1) those dominated by the bulge component, (2) those dominated by a disc component, (3) those which host a classical bulge+disc (‘B+D’) configuration, and others that do not fit these categories. For the purposes of this work we rely on profile types 1 and 3. For a bulge within a disc, we require that the galaxy be classified as a profile type 3. However, it is unclear in the profile fitting whether a pure spheroid system is best fitted by either a single bulge component (type 1) or B+D configuration (type 3). To ensure we are correctly selecting the

Table 1. Selection criteria and subsample sizes.

Quantity	pS	B+D	N(pS)	N(B+D)
S11 sample	n/a		1,123,718	1,123,718
In M14	n/a		656,797	656,797
$\mu_{50,r}$	≤ 23.0 mag arcsec $^{-2}$		654,306	654,306
<i>specclass</i>	2		652,748	654,306
<i>z</i>	0.005 – 0.2		615,719	617,264
<i>prcflag</i>	0		615,719	617,264
Δ_{B+D}	$< 3\sigma$		613,661	615,203
P_{pS}	0.32 – 1.0	0.0 – 0.32	429,418	185,034
Profile Type	1 or 3	3	341,993	170,544
$(B/T)_r$	> 0.5	> 0.0	187,227	170,544
<i>i</i>	n/a	$\leq 60^\circ$	187,227	104,218
$R_{e,kpc}$	> 0.0	$< 1.67R_{d,kpc}$	187,227	104,065
<i>e</i>	< 0.6	< 0.6	171,243	76,012

single-component spheroids and not including the B+D systems, we use the F -test probability (P_{pS}) calculated in S11 which indicates whether a given galaxy is better fitted with the pure Sérsic (‘pS’) model rather than the B+D model. This image modelling was originally performed using the SDSS *gr* images but has since been extended to the *ugriz* filter set to compute galaxy, bulge and disc stellar masses as described in M14. Therefore, the distinction between pure spheroids and bulges is made on the basis of P_{pS} , the profile type, and the *r*-band bulge fraction $((B/T)_r)$. As shown in figure 12 of S11, the combined criteria $0.0 \leq P_{pS} < 0.32$ and $(B/T)_r > 0$ select galaxies for which two-component fitting is required, and the combined criteria $0.32 \leq P_{pS} \leq 1.0$ and $(B/T)_r > 0.5$ select single-component galaxies. The profile type further refines the sample and ensures that the P_{pS} cut is indeed a physical representation of the light profile.

The remaining three selection criteria are disc inclination i , ellipticity e ($e \equiv 1 - \frac{b}{a}$) and effective radius $R_{e,kpc}$. Internal extinction can have a significant impact on measured structural parameters (Pastrav et al. 2013). Given that our bulge subsample was still quite large at this point, we opted to keep only bulges in face-on ($i \leq 60^\circ$) galaxies to improve the quality of this subsample. One difficulty with bulge+disc decompositions of galaxy images is that strong bars can be mistaken for bulges. The signature of this problem is a very high bulge ellipticity. Selecting galaxies with $e < 0.6$ is sufficient to remove bars from the bulge subsample. Finally, we required that the bulge effective radius be smaller than the disc. Our selection criteria¹ are summarized in Table 1.

2.2 Analysis

We build our mass-size relations using the stellar mass (M_*), the maximum volume sampled (V_{max}), and the bulge or spheroid radius R_e in kiloparsecs. The radii given in S11 are measured along the semimajor axes of the galaxies. We circularize these radii using the well-known relation

$$R_{e,circ} = R_{e,sma} \sqrt{1 - e}, \quad (1)$$

¹ These criteria do not introduce any differences in the magnitude distribution between the two subsamples.

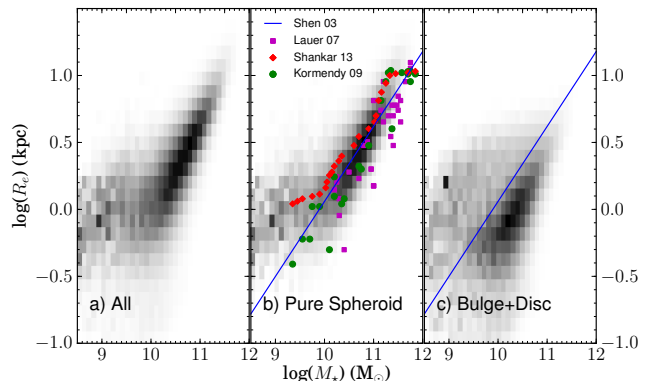


Figure 1. The mass-size relation for (a) the entire sample; (b) the B+D subsample; and (c) the pure spheroid subsample using the V_{max} -corrected space density of our subsamples. Data from a number of previous works (Shen et al. 2003; Lauer et al. 2007; Kormendy et al. 2009; Shankar et al. 2013) are overplotted in the middle panel. Stellar masses for the Lauer et al. (2007) and Kormendy et al. (2009) data are adopted from Hopkins et al. (2009b). The lines from Shen et al. (2003) represent their best fitting curve to their early-type data set, while the Shankar et al. (2013) points represent the median of the distribution of their early-type galaxies.

$R_{e,circ}$ is hereafter simply denoted R_e . The stellar masses are taken from M14. They are estimated from the comparison of the galaxies’ *ugriz* spectral energy distributions with a large grid of photometric templates which encompasses a range of ages, metallicities, star-formation histories and dust contents. This grid is generated from the Flexible Stellar Population Synthesis code (Conroy et al. 2009) in conjunction with a Chabrier initial mass function (Chabrier 2003). This methodology was applied independently to both bulges and discs, deriving the masses from the flux in the regions identified by the S11 decompositions. The errors are typically ~ 0.15 – 0.2 dex, and include the statistical uncertainties from the total fluxes and bulge-to-total ratios measured by S11.

Figure 1 shows the distributions in the mass-size plane of the entire sample, the B+D subsample, and the pS subsample. Both subsamples show a well-defined trend in the mass-size relation, with little scatter (in particular the pS subset). However, there is a large amount of scatter at the low mass end in the B+D subsample. It is apparent that both subsamples do *not* have similar trends, as the majority of B+D systems tend to have smaller sizes for a given mass than their pS counterparts. To compare to previous work, the observed mass-size data from Shen et al. (2003), Lauer et al. (2007), Kormendy et al. (2009), and Shankar et al. (2013)² have been included in the middle panel of Figure 1. Although the distributions do not line up exactly, it is apparent that the spheroid subsample is very similar to the previous measurements. We see the same flattening in the bulge mass-size relation at low masses as reported in Shankar et al. (2013).

² We adopt the stellar masses derived in Hopkins et al. (2009b) for the Lauer et al. (2007) and Kormendy et al. (2009) data.

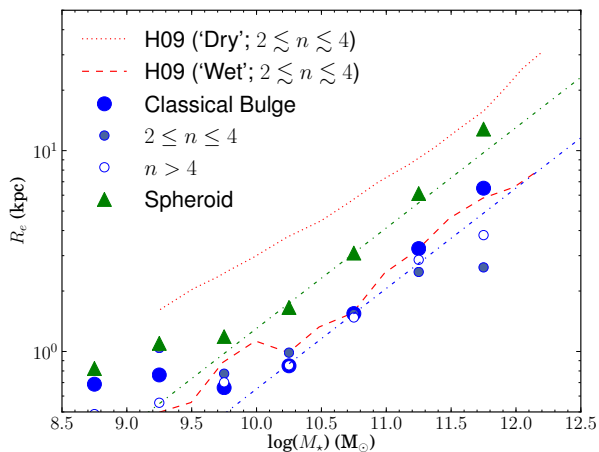


Figure 3. Stellar mass-size relations for bulges (blue circles) and spheroids (green triangles) using the median sizes shown in Figure 2. The smaller circles represent the mass-size relation using different cuts in the Sérsic index of the bulge. Due to the large number of galaxies within each bin, the standard errors are much smaller than the data points and thus are not plotted. The ‘no dissipation’ (or ‘dry’; dotted line) and ‘no dry’ (or ‘wet’; dashed line) merger models from Hopkins et al. (2009b) are shown by red lines, for which galaxies typically have $2 \lesssim n \lesssim 4$. For masses above $\sim 10^{10} M_{\odot}$, the slope of the pure spheroid mass-size relation seems to follow models that do not include dissipation, whereas the B+D galaxies (regardless of n) follow models without dry mergers or include dissipation. The green and blue dash-dotted lines represent lines of constant surface density of stars ($\log(R_e) \propto 0.5\log(M_{\star})$) with $\Sigma = 5.9 \times 10^9$ and $2.4 \times 10^{10} M_{\odot} \text{ kpc}^{-2}$ respectively.

In order to characterize the mass-size relation, both subsets were split into seven equally spaced stellar mass bins, and the size functions of each bin were computed and are shown in Figure 2. We calculate the V_{max} -weighted median size³ (where V_{max} is the maximum volume over which a galaxy can be observed from the M14 catalogues) for each mass bin. Although the scatter for bulges in the lower mass bins is not quite Gaussian, with an extra tail at smaller radii, a Gauss-Hermite expansion of the size functions (e.g., Abraham & van den Bergh 1995) yields mean sizes that agree with the medians to within 0.05 dex.

3 RESULTS AND DISCUSSION

Using the medians from the size functions (Figure 2), the bulge and pure spheroid mass-size relations are shown in Figure 3. For comparison, two different models from Hopkins et al. (2009b) have also been included⁴. These models investigate the predicted mass-size relation at $z = 0$ by: (i) excluding mergers with dissipation (treating gas particles

like stars), and (ii) excluding dry mergers. These two extreme cases produce size mass relations that are parallel to one another, but where the sizes of the bulges in dry mergers are larger than in the gas-rich case. The existence of two distinct mass-size relations in the data, that are also parallel, yet offset, is strong evidence that bulges and pure spheroids form from different types of mergers. *Bulges are not simply pure spheroids wrapped in discs.* This is in agreement with previous studies (Gadotti 2009; Gadotti & Kauffmann 2009; Laurikainen et al. 2010), although our work has a more rigorously defined sample of bulges and spheroids and exceeds the sample sizes of previous works by at least an order of magnitude.

The Hopkins et al. (2009b) models show a large spread in the Sérsic index (predominantly between $2 \lesssim n \lesssim 4$) for the progenitor bulge-like structures. To test the effects of assuming a classical B+D decomposition over a free Sérsic index+disc profile, Figure 3 shows the mass-size relation for bulges with Sérsic within two bins ($2 \leq n \leq 4$ and $n > 4$; blue grey and unfilled circles, respectively) from the S11 catalogue. The masses were derived using the g-r colours in Dutton (2009) as M14 did not derive masses for these free n fits. Overall, there is no great difference between assuming $n = 4$ or adopting a best fitting n for the bulge⁵ with this data set, therefore we continue to use $n = 4$ to represent the populations of bulges.

The first remarkable feature of these relations is their behaviour at masses higher than $\sim 10^{10} M_{\odot}$. The two relations are clearly shifted with respect to each other, with pure spheroids being $1.4\times$ larger than bulges at a fixed stellar mass. This offset is so constant over the mass range $10^{10} M_{\odot} < M_{\star} < 10^{12} M_{\odot}$ that both relations would lie directly on top of each other if this shift were applied to the bulges. They almost follow lines of constant stellar mass surface density ($\log(R_e) \propto 0.5\log(M_{\star})$) in contrast to the virial theorem, which at fixed velocity dispersion, would have $\log(R_e) \propto \log(M_{\star})$. The ‘no-dry’ (‘wet’) merger model of Hopkins et al. (2009b) reproduces the mass-size relation of bulges very well, but neither model is a good match overall to the pure spheroid mass-size relation. The observed relation of pure spheroids approaches the ‘no dissipation’ (‘dry’) model at the highest stellar masses but falls significantly below it for $\log M_{\star} < 11.5$. Clearly, the process that led to the formation of the pure spheroids was not entirely dissipationless, and was therefore likely a mix of wet and dry mergers. This is consistent with Nipoti et al. (2012) who found that present-day, massive early-type galaxies could not have formed entirely through dry merging. Indeed, Kaviraj et al. (2012) and Shabala et al. (2012) have recently identified a specific sample of elliptical galaxies with enhanced star formation rates and nuclear activity that they propose to be the result of a merger.

The second notable feature of these relations is the flattening of size with decreasing mass below $\sim 10^{10} M_{\odot}$. This flattening was also observed by Shankar et al. (2013), and, although they attributed this flattening to a lack of dissipation, none of the Hopkins et al. model curves reproduces this

³ Each galaxy was volume-weighted by V_{max}^{-1} to account for the fact that more luminous galaxies are over-represented in magnitude-limited samples compared to fainter ones.

⁴ The ‘no dissipation’ and ‘no dry’ models from Hopkins et al. (2009b) are relabelled as ‘dry’ and ‘wet’ (respectively) to clarify which merger types are dominating in the models.

⁵ Despite the apparent disagreement between the mass-size relations for the classical bulge and free n fits for the highest mass bin in Figure 3, the points agree within the 1σ range.

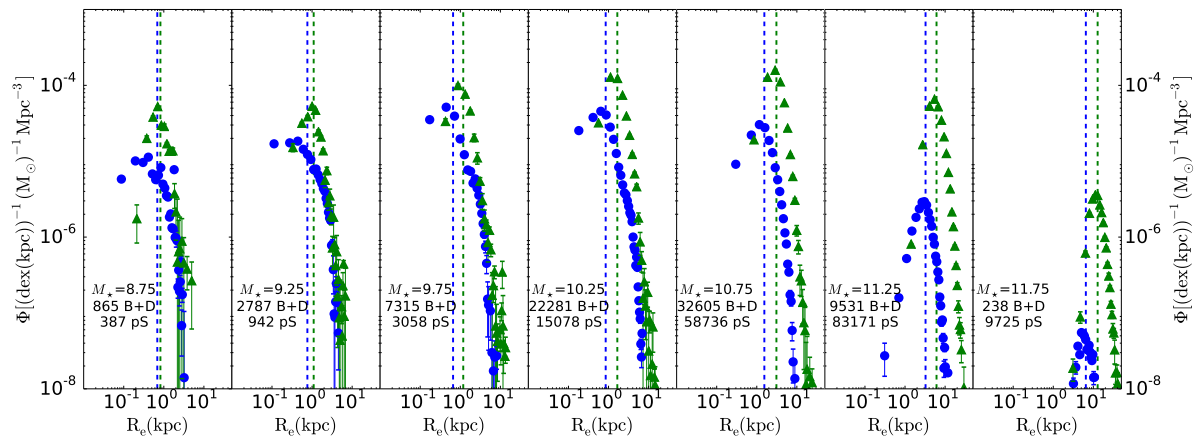


Figure 2. Size functions in bins of spheroid stellar mass. The green triangles and blue circles are the spheroid and bulge subsamples, respectively. The centre of the mass bin is displayed at the bottom of each panel, along with the total number of galaxies in each subsample. The error on each point is generated via a bootstrap method. The vertical dashed lines mark the V_{max} -weighted median values of the distributions.

behaviour well. Bulge formation through secular evolution is expected to play a larger role at lower bulge masses and may be responsible for this flattening of the bulge mass-size relation, but it obviously cannot affect the pure spheroid relation in any way. Either dry mergers must dominate the formation of low mass pS galaxies (Shankar et al. 2013), or another process must be taking place.

Our bulge and pure spheroid mass-size relations and their observed features point towards a picture in which spheroids do emerge from a hierarchical mass assembly process driven by mergers. However the amount of dissipation, i.e., the amount of gas present in these mergers, leaves a distinctive signature on their present-day sizes and masses.

4 CONCLUSION

Using large catalogues of bulge+disc structural parameters and stellar masses for galaxies in the SDSS DR7 Legacy Area, we quantitatively defined two subsamples of galaxy spheroids to distinctly select pure spheroids and bulges with identical properties other than bulges being embedded in disks. These two subsamples are used to study the relation between their size and stellar mass. We found that these subsamples had distinct mass-size relations, which indicates that bulges are not simply present day, pure spheroids wrapped in discs. At stellar masses above $\sim 10^{10} M_{\odot}$, the relations are parallel but shifted by a factor of 1.4 in size at a fixed stellar mass. Bulges follow a mass-size relation consistent with a ‘wet’ merger model, and the relation for pure spheroids indicates a combination of ‘wet’ and ‘dry’ mergers. At stellar masses below $\sim 10^{10} M_{\odot}$, both relations exhibit a flattening in size with decreasing mass that is not reproduced at all by theoretical models. A comparison between our observed relations and theoretical models suggest that dissipation leaves a distinctive signature on the mass-size relations of bulges and pure spheroids.

ACKNOWLEDGEMENTS

We thank Philip Hopkins for graciously providing us with his merger models.

REFERENCES

- Abadi, M. G. et al. 2003, ApJ, 591, 499
- Abazajian, K. et al. 2009, ApJS, 182, 543
- Abraham, R. G., & van den Bergh, S. 1995, ApJ, 438, 218
- Agertz, O. et al. 2011, MNRAS, 410, 1391
- Auger, M. W. et al. 2010, ApJ, 724, 511
- Bender, R., Burstein, D., & Faber, S. M. 1992, ApJ, 399, 462
- Borson, T. 1981, ApJS, 46, 177
- Brooks, A. M. et al. 2011, ApJ, 728, 51
- Burstein, D., Bender, R., & Faber, S. M. 1997, AJ, 114, 1365
- Cappellari, M. et al. 2011, MNRAS, 416, 1680
- Cappellari, M. et al. 2013, MNRAS, 432, 1862
- Chabrier, G. 2003, PASP, 115, 763
- Ciotti, L., Lanzoni, B., & Volonteri, M. 2007, ApJ, 658, 65
- Ciotti, L., & van Albada, T. S. 2001, ApJ, 552, L13
- Conroy, C., White M., & Gunn, J. E. 2009, ApJ, 708, 58
- Courteau, S., de Jong, R. S., & Broeils, A. H. 1996, ApJ, 457, L73
- de Jong, R. 1996, A&A, 313, 45
- Djorgovski, S., & Davis, M. 1987, ApJ, 313, 59
- Dutton, A. A. 2009, MNRAS, 396, 121
- Fall, S. M., & Efstathiou, G. 1980, MNRAS, 193, 189
- Freeman, K. C. 1970, ApJ, 160, 811
- Gadotti, D. A. 2009, MNRAS, 393, 1531
- Gadotti, D. A., & Kauffmann, G. 2009, MNRAS, 399, 621
- Governato, F. et al. 2007, MNRAS, 374, 1479
- Graham, A. W., & Worley, C. C. 2008, MNRAS, 388, 1708
- Guo, Q. et al. 2011, MNRAS, 413, 101
- Hopkins, P. F. et al. 2009a, ApJ, 691, 1168
- Hopkins, P. F. et al. 2009b, ApJ, 691, 1424
- Kanwar, A. et al. 2008, ApJ, 682, 907

- Kaviraj, S. et al., 2012, MNRAS, 435, 1463
Kent, S. M., 1985, ApJS, 59, 115
Kormendy, J., & Bender, R. 2012, ApJS, 198, 2
Kormendy, J. et al. 2009, ApJS, 182, 216
Krajnović, D. et al. 2012, MNRAS, 432, 1768
Lackner, C. N. & Gunn J. E. 2012, MNRAS, 421, 2277
Laurikainen, E. et al. 2010, MNRAS, 405, 1089
Lauer, T. R. et al. 2007, ApJ, 664, 226
Meert, A. et al. 2013, MNRAS, 433, 1344
Mendel, J. T. et al. 2014, ApJS, 210, 3
Mo, H.J., Mao, S., & White, S.D.M. MNRAS, 295, 319
Nipoti, C. et al. 2012, MNRAS, 422, 1714
Nipoti, C., Treu, T., & Bolton, A. S. 2009, ApJ, 703, 1531
Pastrav, B. A. et al. 2013, A&A, 557, 137
Peng, C. et al. 2002, AJ, 124, 266
Robertson, B. et al. 2006, ApJ, 641, 21
Scannapieco, C. et al. 2011, MNRAS, 417, 154
Scarlata, C., et al. 2007, ApJS, 172, 494
Shabala, S. S, et al. 2012, MNRAS, 423, 59
Shankar, F. et al. 2013, MNRAS, 428, 109
Shen, S. et al. 2003, MNRAS, 343, 978
Simard, L. et al. 2002, ApJS, 142, 1
Simard, L. et al. 2011, ApJS, 196, 11
Taranu, D. S., Dubinski, J., & Yee, H . K. C. 2013, ApJ,
778, 61